ORNL/TM-2020/1859

Theoretical Yields for ^{188}W Production in the High Flux Isotope Reactor

J. R. Griswold
V. Bautista
R. Copping
S. Mirzadeh

December 2020

OAK RIDGE NATIONAL LABORATORY
MANAGED BY UT-BATTELLE FOR THE US DEPARTMENT OF ENERGY

ORNL/TM-2020/1859

Radioisotope Science and Technology Division

THEORETICAL YIELDS FOR ^{188}W PRODUCTION IN THE HIGH FLUX ISOTOPE REACTOR

J. R. Griswold
V. Bautista
R. Copping
S. Mirzadeh

December 2020

Prepared by
OAK RIDGE NATIONAL LABORATORY
Oak Ridge, TN 37831-6283
managed by
UT-BATTELLE, LLC
for the
US DEPARTMENT OF ENERGY
under contract DE-AC05-00OR22725

CONTENTS

LIST OF FIGURES

LIST OF TABLES

ACRONYMS

EABD	Experiment Authorization Bases Document
ENDF	Evaluated Nuclear Data Library
EOB	End of Bombardment
GUI	Graphical User Interface
HFIR	High Flux Isotope Reactor
HFIRCON	HFIR CONtroller code
JEFF	Joint Evaluated Fission and Fusion
MCNP	Monte Carlo N-Particle code
NIDC	National Isotope Development Center
ORIGEN	Oak Ridge Isotope Generation code
TRRH	Target Rod Rabbit Holder

ABSTRACT

Accurately predicting the production yield of ^{188}W and ^{191}Os from enriched ^{186}W metal rings irradiated in HFIR is not straightforward. Two key factors can lead to significant uncertainty or inaccuracy in yield predictions:

- The effect of neutron flux depression in the dense tungsten metal target.
- Inaccuracy of the currently published ^{187}W thermal neutron absorption cross section.

This manuscript reports the calculated yields for ^{188}W, ^{191}Os, and total osmium mass for the NM-888 target that was irradiated in High Flux Isotope Reactor (HFIR) Cycles 487 and 488. Three different yield calculation methods were used and are described herein. The results are presented in terms of total yield and in terms of yield per target mass. This allows for an approximate estimation of yields for future targets of varying mass loading but with similar irradiation profiles. For more accurate prediction yields, target-specific models that account for target loading, target positioning within HFIR, and accurate HFIR cycle data are required.

1. BACKGROUND

Tungsten-188 is produced through the irradiation of enriched ^{186}W in the High Flux Isotope Reactor (HFIR). This requires two neutron captures, one in the ^{186}W target material and one in the short-lived intermediary nuclide, ^{187}W ($t_{1/2}$ = 24.00 hr). The relevant radionuclides and production pathways are shown in Figure 1. Tungsten-188 production rabbits are typically irradiated for two cycles in HFIR to produce enough ^{188}W to ship 10–12 Ci after chemical processing.

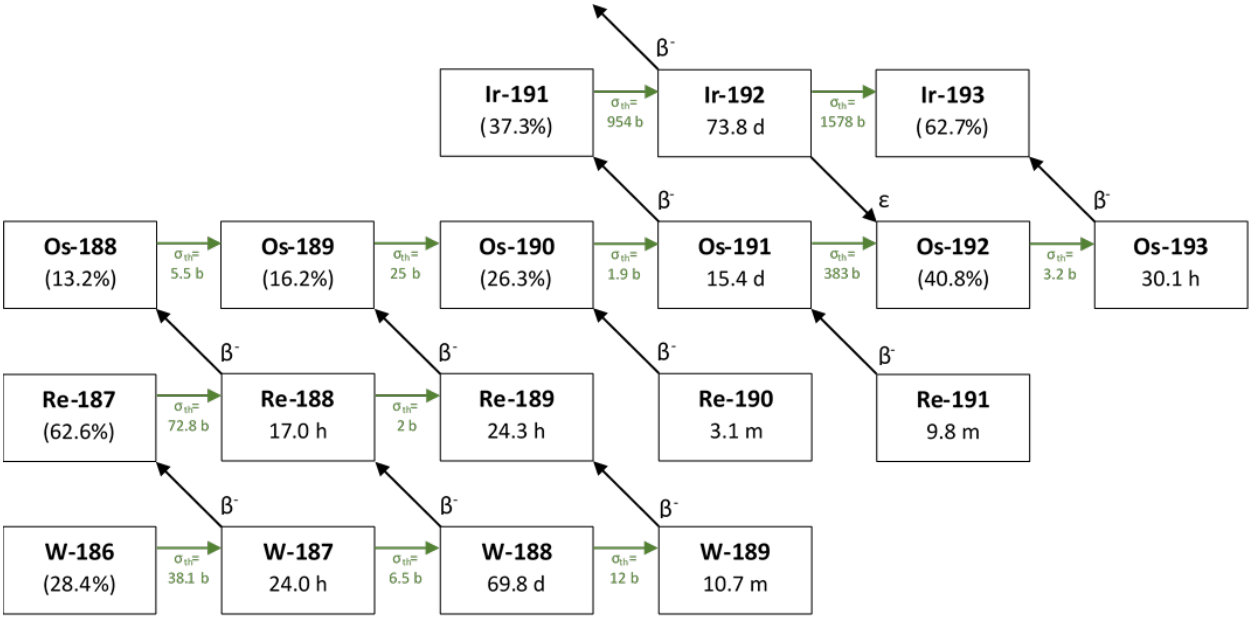

Figure 1. Relevant nuclides for the production of ^{188}W in HFIR.

In the target fabrication process, enriched ^{186}W metal rings are loaded into a standard finned rabbit. The rabbit drawing (N3E020977A036 Rev 0) and assembly drawing (JLM02142007-1 Rev 0) can be found in Appendix A. As shown on the assembly drawing, a maximum tungsten mass of 4.833 g can be loaded into each rabbit. In practice, this equates to eight tungsten metal rings weighing approximately 600 mg

each. For the recent NM-888 production target, eight metal rings were loaded for a total tungsten mass of 4.7344 g. The dimensions for each of the rings are shown in Table 1. The tungsten feedstock used for this campaign was National Isotope Development Center (NIDC) Lot #146643 and was enriched to 96.95% ^{186}W. The mass assay including impurities is shown in Appendix B.

Table 1. Tungsten Ring Measurements for NM-888.

Ring ID#	Sintered weight (mg)	Sintered height (mm)	Sintered outside diameter (mm)	Sintered inside diameter (mm)	Calculated density (g/cm^3)
6(9/19)	578.2	2.33	6.05	3.84	14.5
8	601.3	2.47	6.04	3.85	14.3
9	595.9	2.46	6.02	3.81	14.2
11	597	2.48	6.02	3.82	14.2
12	598.4	2.5	6.03	3.83	14.0
15	597.7	2.46	6.1	3.8	13.6
17	592.7	2.38	6.08	3.83	14.2
20	573.2	2.28	6.08	3.82	14.3

After fabrication and Experiment Authorization Bases Document (EABD) approval, the rabbit was loaded into position D3-4 of the Target Rod Rabbit Holder (TRRH) region of the HFIR flux trap and irradiated for two cycles, Cycle 487 and Cycle 488. The starting and finishing dates of each cycle are shown below in Table 2. It is important to note that there were some technical difficulties encountered by HFIR Operations staff at the start of Cycle 488, resulting in a short, 2.5-day delay after a very brief low-power start-up, denoted as Cycle 488A. The total accumulated burnup for Cycle 488A was 14.06 MWd over a span of ~7 hours. This equates to ~4 hours at full power. For simplicity of all the simulations described later in this report, Cycle 488A is assumed to operate at ~4 hours at full power instead of ~7 hours at increasing power. This is reflected in Table 2.

Table 2. HFIR Irradiation Parameters for NM-888.

Cycle	Start	End	Duration (d)
487 ON	4/28/20 9:20	5/23/20 11:47	25.1
487 OFF	5/23/20 11:47	6/9/20 16:58	17.2
488A ON	6/9/20 16:58	6/9/20 20:57	0.2
488A OFF	6/9/20 20:57	6/12/20 7:47	2.5
488B ON	6/12/20 7:47	7/7/2020 16:00	25.3
		Total Duration	50.61

2. CALCULATION METHODS

Three different modeling and simulation methods were used to predict the theoretical ^{188}W and ^{191}Os yields in NM-888: HFIRCON, IsoChain, and MCNP6 combined with ORIGEN (MCNP6-ORIGEN). Some general considerations about the assumptions that apply to all three calculation methods should be noted before describing the individual calculation methods.

2.1 DENSITY OF TUNGSTEN METAL

Tungsten metal has a theoretical density of 19.3 g · cm^{-3}, which leads to significant neutron flux depression at the center of the target mass during irradiation. To offset this effect, the ^{188}W production targets are fabricated in the form of tungsten metal rings. This allows for less neutron flux depression and a higher specific activity of ^{188}W product [1]. However, the neutron flux at the center of the rings is still significantly lower than the neutron flux on the outside of the rings. The HFIRCON method and the MCNP6-ORIGEN method described below can account for this neutron flux depression, while the IsoChain method—a basic, two-group Bateman calculation—cannot. Additionally, each pressed and sintered tungsten ring varies in its measured density and void fraction, as shown in Table 1. For each of the calculation methods described in subsequent sections of this work, the average density of the tungsten rings was applied to the entire stack for simplicity.

2.2 $^{187}W(N, Y)^{188}$ REACTION CROSS SECTION

Another issue that must be addressed when performing these calculations is the inaccuracy of the currently accepted ^{187}W thermal neutron absorption cross section. The *Atlas of Neutron Resonances* [2] lists the cross section as 64 b and the resonance integral as 2760 b. These data originally come from a 1966 ORNL annual report [3] that does not include any technical details. A recent publication by Ersoz et al. [4] reevaluated the ^{187}W cross section and concluded that the previously reported thermal cross section was incorrect by a factor of 10. Table 3 shows both values along with the other relevant cross section data for the production of ^{188}W and ^{191}Os in HFIR. It is important to note that HFIRCON is the only calculation method described in this report that currently does not allow users to modify the cross section library used within the calculation.

Table 3. Selected Cross Sections Used in IsoChain Relevant to the Production of ^{188}W and ^{191}Os through Thermal Neutron Absorption.[a]

Reaction cross section	Thermal (b)	Resonance integral (b)	Source
$^{186}W(n,\gamma)$	38.1	480	Mughabghab [2]
$^{187}W(n,\gamma)$	64[a]	2760[b]	Mughabghab [2]
$^{187}W(n,\gamma)$	6.5[b]	279.5[c]	Ersoz [4]
$^{188}W(n,\gamma)$	12	Unknown	Mirzadeh [5]
$^{188}Os(n,\gamma)$	5.5	116	Mughabghab [2]
$^{189}Os(n,\gamma)$	25	736	Mughabghab [2]
$^{190}Os(n,\gamma)$	1.93	4.77	Mughabghab [2]
$^{190}Os(n,\gamma)^{191m}Os$	9.03	25.4	Mughabghab [2]
$^{191}Os(n,\gamma)$	383	Unknown	Mughabghab [2]
$^{192}Os(n,\gamma)$	3.16	7.45	Mughabghab [2]

[a]All transitions are to the ground state unless notated otherwise.
[b]Value used in default IsoChain and MCNP6-ORIGEN calculations.
[c]Value used in corrected IsoChain and MCNP6-ORIGEN calculations.

2.3 HFIRCON

The HFIRCON (HFIR CONtroller) code is a high-fidelity code system used for depletion analyses of targets and fuel within HFIR. It combines the codes LAVAMINT, ORNLTN/MCNP5, ADVANTG, and ORIGEN (Oak Ridge Isotope Generation code) to effectively combine radiation transport with depletion

analyses [6]. Users can define their specific target geometries within existing models of the HFIR. Several models of the HFIR have been extensively documented to date such as the Cycle 400 model and the representative model, both of which have been studied using a simplified and explicit modeling of the fuel elements [7]. Figure 2 shows a cross section of the MCNP (Monte Carlo N-Particle code) model with the tungsten ring target loaded into position D3-4 of the flux trap. HFIRCON will iteratively determine neutron flux and target activation throughout the cycle as fuel and target depletion occur. In theory, the iterative flux and depletion calculations should generate a more accurate, time-dependent neutron flux and target activation than other methods described in this report. However, the increased precision gained with this method comes at the cost of computational resource requirements. HFIRCON requires a parallel computing system to run efficiently. Additionally, the current version of HFIRCON only allows multi-group cross sections to be modified by the code's developers and does not allow users to modify cross sections. The cross sections included with HFIRCON are from the default ORIGEN library that derives its data from the latest Evaluated Nuclear Data File (ENDF) library. If the cross section data for specific materials and processes are not available in ENDF, it uses the Joint Evaluated Fission and Fusion 3.0/A (JEFF 3.0/A) library as a secondary library [8].

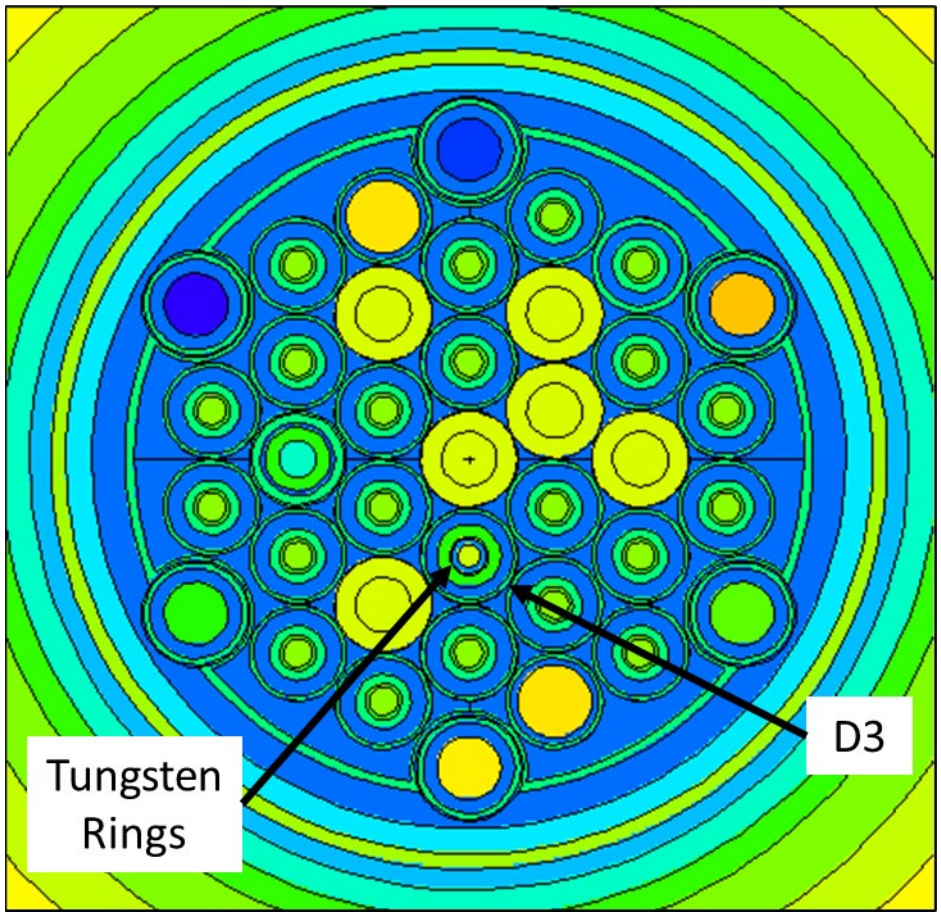

Figure 2. Axial view of MCNP6 HFIR Cycle 400 model with the tungsten metal ring rabbit loaded in radial position D3 of the HFIR flux trap.

2.4 ISOCHAIN

IsoChain is a simulation code written in the JAVA programming language that uses the Bateman Equations to transmute and decay radionuclides based on user-defined parameters such as irradiation time, flux, thermal-to-epithermal flux ratio, and target composition [9, 10]. In the original development of

the code, a default two-group cross section library was included based on available data from an older version of the *Atlas of Neutron Resonances* [11]. The two-group cross section data can easily be modified as needed within the IsoChain Graphical User Interface (GUI). The selected cross section data used in this report to modify the existing IsoChain cross section library are shown in Table 3, and the full cross section data are shown in Appendix C. The IsoChain input flux is defined as the thermal flux and the thermal-to-epithermal ratio. These values are always defined by the user. In the case of this simulation, the input flux was 2×10^{15} n·cm^{-2}·s^{-1} and the thermal-to-epithermal flux ratio was 30. These values were measured for position 4 within the HFIR hydraulic tube (position B3 within the flux trap) [12]. The flux at this hydraulic tube position should be relatively similar to the flux at D3-4, the position for the NM-888 tungsten metal ring target. One of the main limitations of IsoChain in comparison with the other methods discussed in this report is the inability to account for neutron flux depression within the target. IsoChain is geometry independent and only calculates the transmutation and decay of the target material based on the total number of atoms present. In effect, IsoChain assumes that all targets are infinitely thin. This is a significant limitation when attempting to account for the neutron absorption within a dense target like the tungsten metal ring target.

2.5 MCNP6-ORIGEN

The third method used combines the HFIR Cycle 400 MCNP model mentioned above to determine the average flux throughout the target. Using this method, the calculated flux can only be determined at a single point in time. This is typically either at the beginning of the cycle or the end of the cycle. In this report, the beginning of the cycle model was used. Just as with HFIRCON, the target location within the HFIR flux trap as well as target composition can be defined in the MCNP input deck. The generated output from MCNP6 is a multigroup neutron flux that is dependent on target composition and density and target location. The calculated flux is then manually imported into the SCALE module ORIGEN to activate and deplete the target. Flux-dependent, effective cross sections for ORIGEN that are representative of the target were generated using COUPLE, the library management code for ORIGEN. The COUPLE module weights an infinitely dilute cross-section by the tallied flux – generated by MCNP6 in this case – and then collapses it to an effective one-group cross section. The higher the energy fidelity in the collapsed data, the more accurate the effective cross section is. COUPLE allows for the user to input custom one-group effective cross sections. If the user does not input effective cross sections, the default ORIGEN library described in Section 2.3 is used to generate effective cross sections.

3. CALCULATION RESULTS AND DISCUSSION

The target details shown in Table 1 and the irradiation parameters displayed in Table 2 were used to generate the activity yield curves for ^{188}W and ^{191}Os shown in Figure 3 and Figure 4, respectively. These values are also shown in Table 4. For the IsoChain and MCNP6-ORIGEN, two separate calculations were performed. The first calculation, notated as "default," used the original value for the ^{187}W absorption cross section from Gillette et al. [3]. The second calculation, denoted as "corrected," used the updated ^{187}W cross section from Ersoz et al. [4]. The HFIRCON calculation is noted as "default" because, as described above, the cross section library cannot be modified by users.

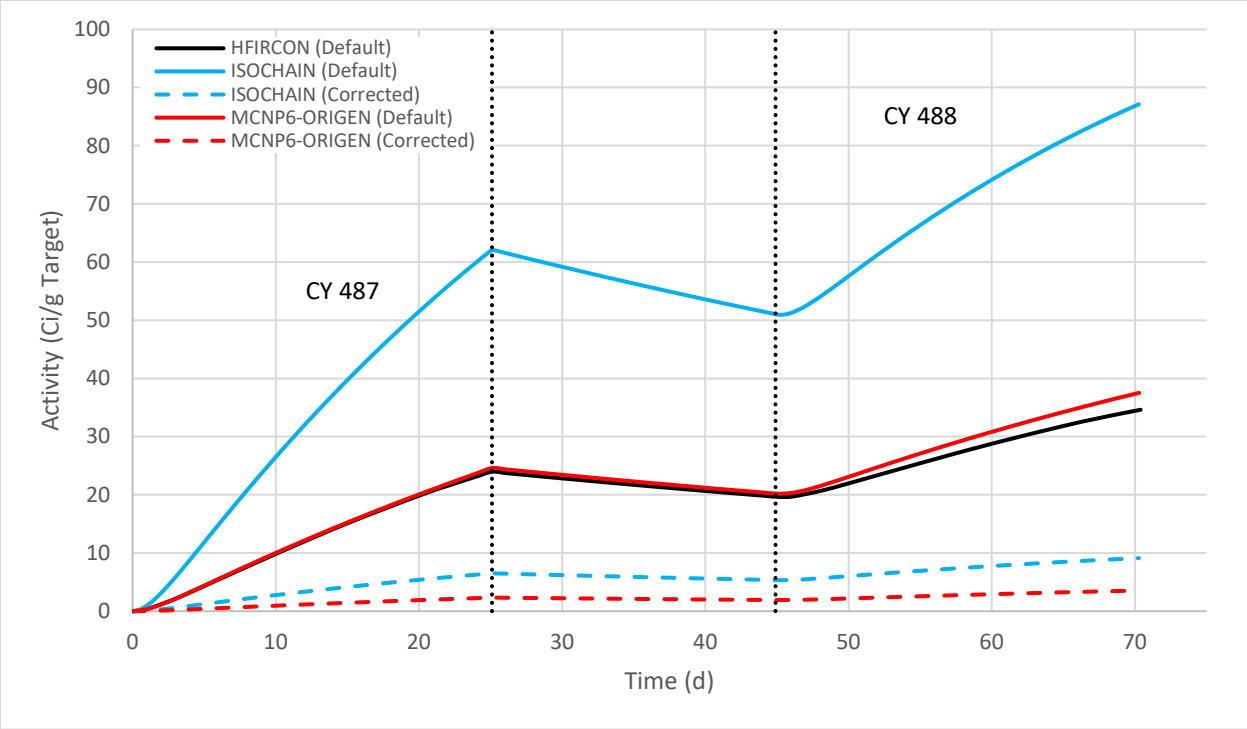

Figure 3. Calculated production of ^{188}W in HFIR cycles 487 and 488. Units are in Ci per gram of irradiated tungsten metal.

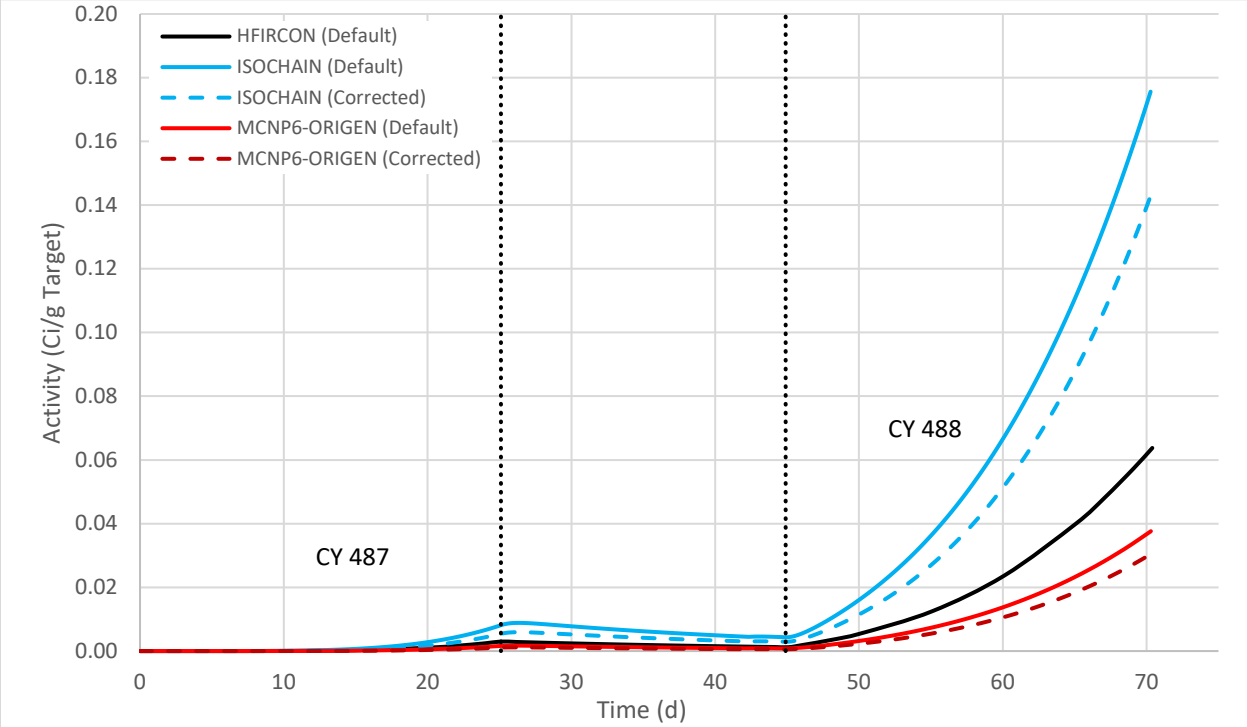

Figure 4. Calculated production of ^{191}Os in HFIR cycles 487 and 488. Units are in Ci per gram of irradiated tungsten metal.

Table 4. Calculated ^{188}W and ^{191}Os Yields at End of Bombardment for NM-888 with Selected Methods.

Method	^{188}W Activity (Ci)	^{191}Os Activity (Ci)	Total osmium mass (mg)
HFIRCON	164	0.30	190
ISOchain (Default)	413	0.83	520
ISOchain (Corrected)	43.2	0.68	519
MCNP6-ORIGEN (Default)	178	0.18	166
MCNP6-ORIGEN (Corrected)	16.8	0.14	163

As expected, the highest and most conservative values calculated for ^{188}W, ^{191}Os, and total osmium mass are from the IsoChain default calculation that uses the higher cross section value for ^{187}W. It is important to note that this value is inflated due to the inability to account for flux depression in IsoChain. As shown in Figure 4, ^{191}Os production is negligible in the first irradiation cycle because the main pathway to produce ^{191}Os is through neutron absorption in the stable nuclides ^{187}Re and ^{188}Os. The mass of ^{187}Re and ^{188}Os builds up through the decay of ^{187}W and ^{188}W during the decay period between the first and second irradiation cycles.

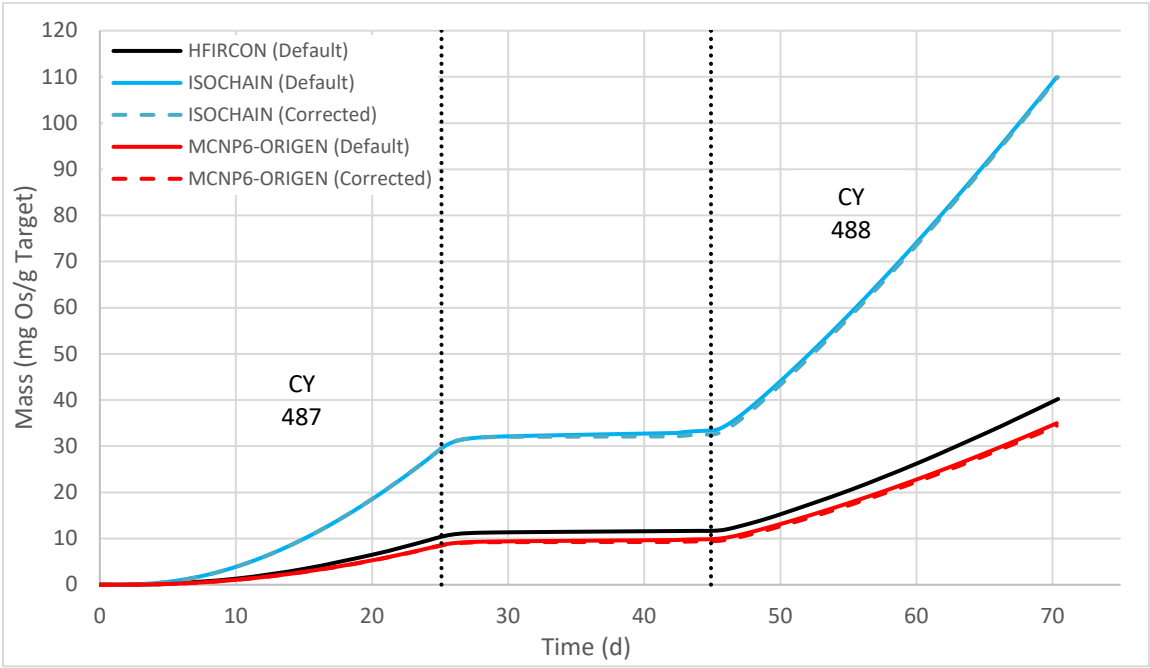

Figure 5. Calculated production of elemental osmium in HFIR cycles 487 and 488. Units are in milligrams of osmium per gram of irradiated tungsten metal.

The total osmium mass generated in this process is important because of the volatility of OsO_4 that is produced during the chemical processing of the irradiated tungsten metal targets. As shown in Figure 5, the magnitude of the ^{187}W cross section has very little effect on the yield of total elemental osmium. For both the IsoChain and MCNP6-ORIGEN calculation methods, the calculations employing the default cross sections and calculations employing the corrected ^{187}W cross section calculate equivalent masses of elemental osmium. The most conservative estimate of osmium mass is generated with the default IsoChain model. As shown in Table 4, this value is estimated to be 520 milligrams of elemental osmium for NM-888 (110 milligrams of elemental osmium per gram of irradiated tungsten metal target).

4. SUMMARY AND CONCLUSIONS

Three different calculation methods were used to determine the production yields of ^{188}W, ^{191}Os, and total elemental osmium in HFIR through the two-cycle irradiation of a rabbit loaded with 4.7344 grams of enriched ^{186}W metal rings. The highest, most conservative yields were calculated using IsoChain with cross sections from the *Atlas of Neutron Resonances* [2]. However, IsoChain assumes an infinitely thin target and does not account for neutron flux depression, and as a result these values are artificially inflated. HFIRCON estimates were typically in between those of IsoChain and MCNP6-ORIGEN. Until HFIRCON developers add an option for user-defined cross sections, the most accurate method to predict yields for the production of ^{188}W in HFIR is the MCNP6-ORIGEN method with user-corrected cross sections. This method can account for the neutron flux depression as well as the inaccuracy of the currently accepted ^{187}W neutron absorption cross section, whereas HFIRCON can only account for neutron flux depression within the target.

5. ACKNOWLEDGMENT

This research is supported by the US Department of Energy Isotope Program, managed by the Office of Science for Nuclear Physics.

6. REFERENCES

1. Garland, M. A., "Neutronic Effects on Tungsten-186 Double Neutron Capture." In *Department of Materials Science and Engineering*. College Park, MD: University of Maryland, 2004.
2. Mughabghab, S. F., *Atlas of Neutron Resonances*. 6th ed. Vol. 2. Amsterdam, Netherlands: Elsevier, 2018.
3. Gillette, J. H., *Review of Radioisotope Program, 1965*. Oak Ridge, TN: Oak Ridge National Laboratory, 1966, p. 5.
4. Ersöz, O. A., et al., "Measurement of neutron capture cross section of ^{187}W for production of ^{188}W," *Applied Radiation and Isotopes* 148 (2019): 191–196.
5. Mirzadeh, S., F. F. Knapp, and R. M. Lambrecht, "Burn-up Cross-Section of ^{188}W," *Radiochimica Acta* 77(1–2) (1997): 99–102.
6. Wilson, S. C., et al., *HFIRCON Version 1.0.5 User Guide*. Oak Ridge, TN: Oak Ridge National Laboratory, 2020.
7. Ilas, G., et al., *Modeling and Simulations for the High Flux Isotope Reactor Cycle 400*. Oak Ridge, TN: Oak Ridge National Laboratory, 2015.
8. Rearden, B.T. and M.A. Jessee, *Scale Code System*. Oak Ridge, TN: Oak Ridge National Laboratory, 2018.
9. Almanza, C.L.J., et al., "IsoChain: a user-friendly, two-group nuclear transmutation and decay code," *Transactions in American Nuclear Society* 95(1) (2006): 441–442.
10. Mirzadeh, S. and P. Walsh, "Numerical evaluation of the production of radionuclides in a nuclear reactor (Part I)," *Applied Radiation and Isotopes* 49(4) (1998): 379–382.
11. Mughabghab, S.F., *Atlas of Neutron Resonances*. 5th ed. Amsterdam, Netherlands: Elsevier, 2006.
12. Mahmood, S.T., et al., *Neutron Dosimetry of the HFIR Hydraulic Facility*. Oak Ridge, TN: Oak Ridge National Laboratory, 1995.

APPENDIX A. RELEVANT DRAWINGS

APPENDIX A. RELEVANT DRAWINGS

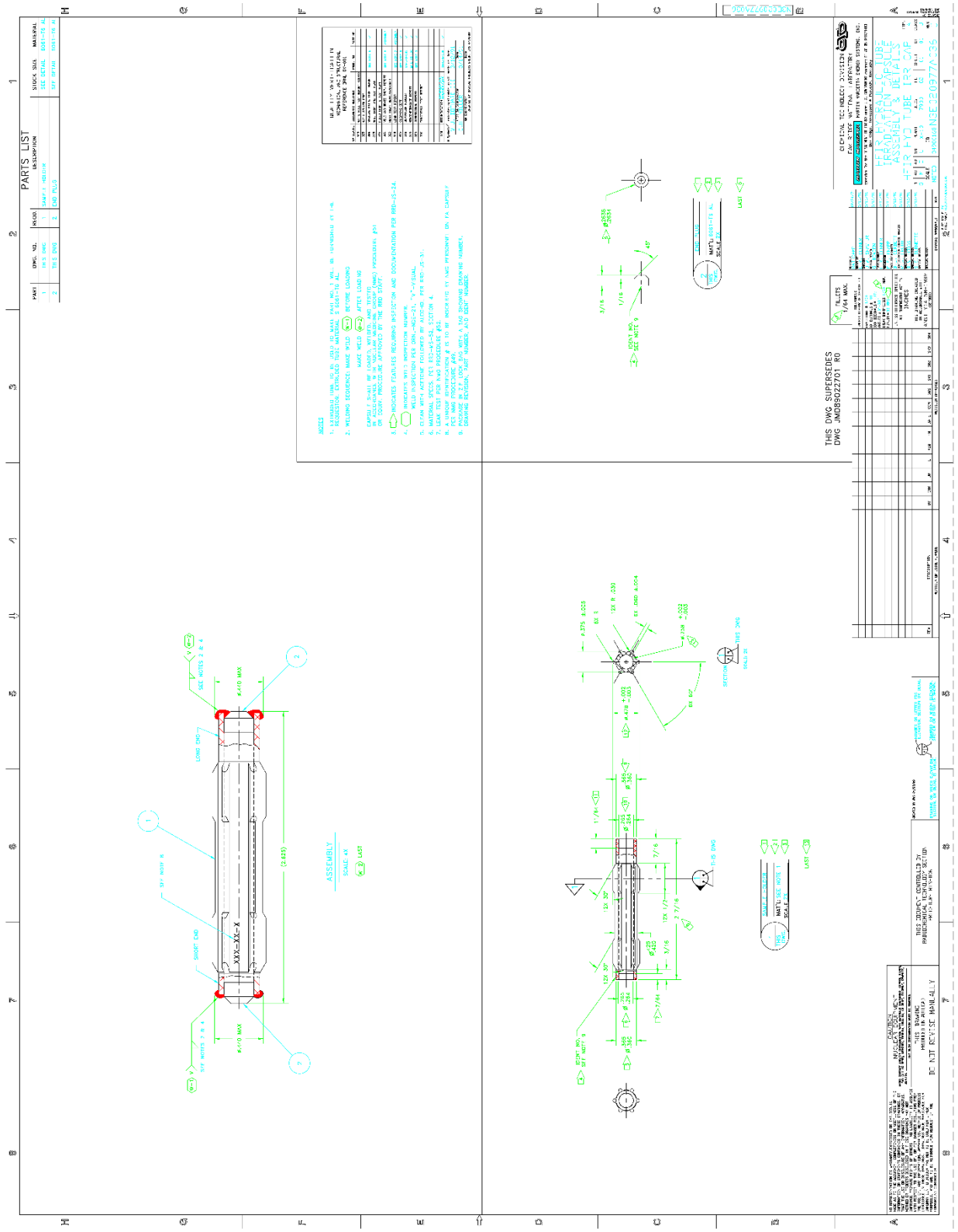

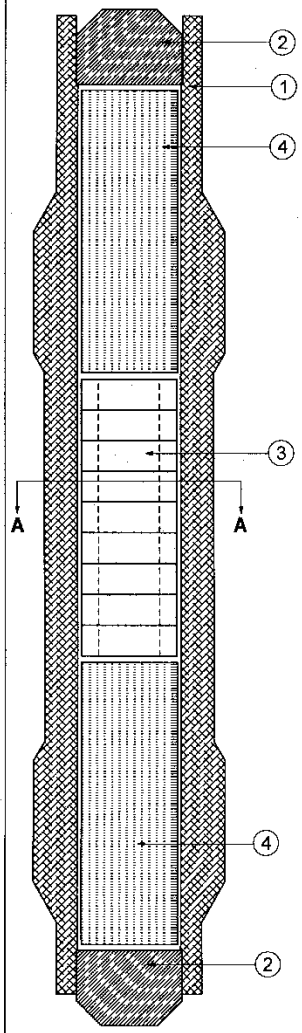

Item	Description	Material	Drawing	Part
1	Housing	Al 6061	N3E020977A036	1
2	End cap	Al 6061	N3E020977A036	2
3	Tungsten ring specimens	Tungsten (0% to 100% enriched in W-186)	This drawing	---
4	Quartz wool	High-purity synthetic quartz wool	This drawing	---

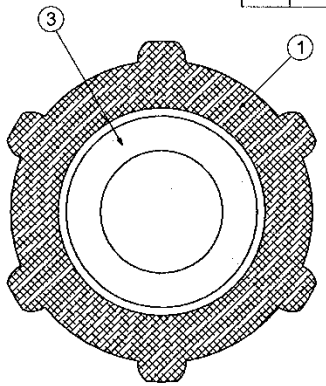

Section A-S

NOTES:

(1) Features indicated by ⟨X⟩ shall be inspected and recorded in accordance with RRD-JS-24.
(2) Individual specimens are optional and interchangeable. A maximum of 4.833 g of specimens per capsule is allowed.
(3) Specimen inner diameter, outer diameter, and total tungsten mass per capsule are critical parameters. Individual specimen height, and number of specimens may vary within these limits.
(4) Amount of quartz wool varies as required by experiment.
(5) Final seal weld must be conducted in a helium environment.
(6) See Drawing N3E020977A036 for welding and assembly instructions.
(7) Specimen inside and outside diameter tolerance is +/- 0.06 mm.

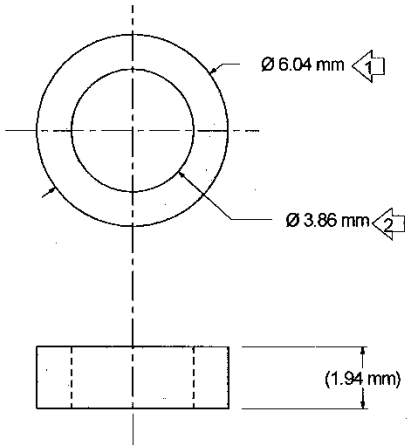

Part 3. Tungsten Ring Specimen

⟨2⟩ Last inspection

Specimen Layout for Tungsten Ring Rabbits

JLM02142007 - 1 Rev 0

Task Leader: J M Maki 2/27/07

Technical Reviewer: D. W. Heatherly 2/27/07

Lead QAS: 2/27/07

RRD Safety: 2/27/07

RRD QA: 2/27/07

APPENDIX B. ICP-MS RESULTS FOR NIDC TUNGSTEN LOT #146643

APPENDIX B. ICP-MS RESULTS FOR NIDC TUNGSTEN LOT #146643

ASSAY

Element: Tungsten
Symbol: W
Isotope: 186
Series: MC
Batch: 146643

ISOTOPIC ANALYSIS

Isotop	Atomic Percen	Precision plus/minus
180	<0.01	0.00000
182	0.76	0.02000
183	0.60	0.01000
184	1.69	0.02000
186	96.95	0.04000

The limits quoted above are an expression of the precision of this measurement only.
The error is estimated at less than 1% from known sources of systematic errors.

SPECTROGRAPHIC ANALYSIS (SSMS)

Element: ppm	Element: ppm	Element: ppm	Element: ppm
Ag: <.4	I: <.2	Rh: <.2	Tc:
Al: 2	In: <.2	Ru: <.6	Te: <.7
As: <.5	Ir: <.6	S: 2	Th <.5
Au: <1	K: 4	Sb: <.4	Ti: 4
B: 9	Li:	Sc: <.3	Tl: <.6
Ba: <.4	Mg: <1	Se: <.3	U: <.5
Be: .7	Mn: .2	Si: 120	V: 460
Bi: <.4	Mo: 3	Sn: <.7	W: MATRIX
Br: <.3	N:	Sr: <.2	Zn: 3
C:	Na: 2	Ta: <2	Zr: <1
Ca: 81	Nb: MASKED		
Cd: <.8	Ni: 2		
Cl: 4	O:		
Co: <.1	Os: <.9		
Cr: 19	P: 30		
Cs: <.3	Pa:		
Cu: 9	Pb: <2		
F: <.4	Pd: <.8		
Fe: 18	Pm:		
Ga: <.2	Po:		
Ge: <.4	Pt: <3		
Hf: <1	Ra:		
Hg: <4	Rb: <.6		
	Re: <2		

LANTHANIDES and ACTINIDES

Am:	La: <.3
Bk:	Lu: <.4
Ce: <.3	Md:
Cf:	Nd: <1
Cm:	Np:
Dy: <1	Pr: <.3
Er: <1	Pu:
Es:	Sm: <1
Eu: <.6	Tb: <.3
Fm:	Y: <.2
Gd: <1	Yb: <1
Ho: <.3	Tm: <.3

* Request No. B-0961; Requisition No. 35150
* Symbols: M - major; T - trace; I - interference; < - less than; <= - less than/equal to; ~ - approximately; nd - not detected; no analyses made in all other cases.
* <- No spectrum line visible. Probably absent, definitely less than value given.
* <T- Present but less than value given.
* The spectrographic results reported herein are semi-quantitative estimates and should not be interpreted or construed to be precise quantitative determinations.

APPENDIX C. COMPLETE ISOCHAIN CROSS SECTION LIBRARY

APPENDIX C. COMPLETE ISOCHAIN CROSS SECTION LIBRARY

Reaction cross section	Thermal (b)	Resonance Integral (b)	Source
$^{180}W(n,\gamma)$	22.3	226	Mughabghab [2]
$^{181}W(n,\gamma)$	9.8	953	Mughabghab [2]
$^{182}W(n,\gamma)$	19.9	602	Mughabghab [2]
$^{183}W(n,\gamma)$	10.4	364	Mughabghab [2]
$^{184}W(n,\gamma)$	1.73	14.7	Mughabghab [2]
$^{185}W(n,\gamma)$	3	183	Mughabghab [2]
$^{186}W(n,\gamma)$	38.1	480	Mughabghab [2]
$^{187}W(n,\gamma)$	64	2760	Mughabghab [2]
$^{187}W(n,\gamma)$	6.5	279.5	Ersoz [4]
$^{188}W(n,\gamma)$	12	Unknown	Mirzadeh [5]
$^{185}Re(n,\gamma)$	112	1739	Mughabghab [2]
$^{186}Re(n,\gamma)$	68.5	Unknown	Mughabghab [2]
$^{187}Re(n,\gamma)$	72.75	294	Mughabghab [2]
$^{187}Re(n,\gamma)^{188m}Re$	2.05	Unknown	Mughabghab [2]
$^{188}Re(n,\gamma)$	2	Unknown	Mughabghab [2]
$^{184}Os(n,\gamma)$	3000	601	Mughabghab [2]
$^{186}Os(n,\gamma)$	80	247	Mughabghab [2]
$^{187}Os(n,\gamma)$	320	473	Mughabghab [2]
$^{188}Os(n,\gamma)$	5.5	116	Mughabghab [2]
$^{189}Os(n,\gamma)$	25	736	Mughabghab [2]
$^{190}Os(n,\gamma)$	1.93	4.77	Mughabghab [2]
$^{190}Os(n,\gamma)^{191m}Os$	9.03	25.4	Mughabghab [2]
$^{191}Os(n,\gamma)$	383	Unknown	Mughabghab [2]
$^{192}Os(n,\gamma)$	3.16	7.45	Mughabghab [2]